# Autocrine fibronectin from differentiating mesenchymal stem cells induces the neurite elongation *in vitro* and promotes nerve fiber regeneration in transected spinal cord injury

Xiang Zeng,[1] Yuan-huan Ma,[1,2] Yuan-feng Chen,[3] Xue-cheng Qiu,[1] Jin-lang Wu,[4] Eng-Ang Ling,[5] Yuan-shan Zeng[1,3,6,7,8]

[1]Key Laboratory for Stem Cells and Tissue Engineering, Sun Yat-sen University, Ministry of Education, Guangzhou 510080, China

[2]Department of Histology and Embryology, Guangdong Medical University, Zhanjiang 524023, China

[3]Department of Histology and Embryology, Zhongshan School of Medicine, Sun Yat-sen University, Guangzhou 510080, China

[4]Department of Electron Microscope, Zhongshan School of Medicine, Sun Yat-sen University, Guangzhou 510080, China

[5]Department of Anatomy, Yong Loo Lin School of Medicine, National University of Singapore, Singapore 117597, Singapore

[6]Institute of Spinal Cord Injury, Sun Yat-sen University, Guangzhou 510120, China

[7]Co-innovation Center of Neuroregeneration, Jiangsu 226019, China

[8]Guangdong Provincial Key Laboratory of Brain Function and Disease, Zhongshan School of Medicine, Sun Yat-sen University, Guangzhou 510080, China

**Abstract:** Extracellular matrix (ECM) expression is temporally and spatially regulated during the development of stem cells. We reported previously that fibronectin (FN) secreted by bone marrow mesenchymal stem cells (MSCs) was deposited on the surface of gelatin sponge (GS) soon after culture. In this study, we aimed to assess the function of accumulated FN on neuronal differentiating MSCs as induced by Schwann cells (SCs) in three dimensional transwell co-culture system. The expression pattern and amount of FN of differentiating MSCs was examined by immunofluorescence, Western blot and immunoelectron microscopy. The results showed that FN accumulated inside GS scaffold, although its mRNA expression in MSCs was progressively decreased during neural induction. MSC-derived neuron-like cells showed spindle-shaped cell body and long extending processes on FN-decorated scaffold surface. However, after blocking of FN function by application of monoclonal antibodies, neuron-like cells showed flattened cell body with short and thick neurites, together with decreased expression of integrin β1. *In vivo* transplantation study revealed that autocrine FN significantly facilitated endogenous nerve fiber regeneration in spinal cord transection model. Taken together, the present results showed that FN secreted by MSCs in the early stage accumulated on the GS scaffold and promoted the neurite elongation of neuronal differentiating MSCs as well as nerve fiber regeneration after spinal cord injury. This suggests that autocrine FN has a dynamic influence on MSCs in a three dimensional culture system and its potential application for treatment of traumatic spinal cord injury. © 2016 Wiley Periodicals, Inc. J Biomed Mater Res Part A: 104A: 1902–1911, 2016.

**Key Words:** fibronectin, mesenchymal stem cells, neurite outgrowth, gelatin sponge scaffold, nerve fiber regeneration

---

---

## INTRODUCTION

The interaction between cells and extracellular matrix (ECM) plays essential roles for cell migration, cell fate determination, forming of tissue-specific functions, tissue repair, oncogenesis, and cell death.[1] To maintain homeostasis, the generation and degradation process of tissue specific ECM must be temporally and spatially regulated to accommodate the needs of cells during different stages and throughout their entire life.[2,3] Stem cells, as early stage of all functional cells, are able to change the microenvironment through the interactions with their niche, while the niche may also support their self-renewal capability, maintain their multipotency, and facilitate differentiation in response to appropriate signals.[4] Studies have shown that mesenchymal stem cells (MSCs) are able to secrete laminin (LN), fibronectin (FN), chondroitin sulfate proteoglycan 2 (CSPG2), collagen type I, III, and V, and various types of proteoglycans[5,6] to the substrate to maintain their stemness. However, once they differentiate, the ECM contents switch to be those supportive to functional daughter cells,[7–9] representing a temporal order as response to genetic changes. To utilize the principle of interaction between stem cells and ECM, one of the strategies for biomaterial construction is to use ECM or ECM pre-coated polymers as scaffolds of stem cells to facilitate tissue-specific cell differentiation.[10–14] Given the fact that ECM molecules have comprehensive interaction during tissue genesis,[15,16] use of ECM compounds for scaffold fabrication should be considered as ideal. It was reported that native cell-free ECM simulated tissue specific microenvironment due to its natural assembly.[9,17] However, adding of ECM components in layers for 3D architecture construction had resulted in various cell behavior changes.[18,19] These findings show that the complication of mutual interaction between cells and ECM is not well understood to date. Hence, microenvironment which captures key features of the unique chemistry, topography and physical properties of a cell's niche-an environment that not only is tissue specific but is strikingly heterogeneous and continuously remodeled over time is now raised as 4D biology,[20] highlighting the dynamic fashion of ECM over time.

Our previous study reported that fibronectin (FN) secreted by MSCs accumulated in a gelatin sponge (GS) scaffold,[21] due to its high affinity to gelatin—a cross link form of collagen, via its gelatin binding domain (GBD).[22] Our finding further suggests that FN and MSCs may have a synergistic effect on angiogenesis when MSC-containing scaffold was implanted *in vitro*,[21] indicating autocrine ECM deposition could affect cell behavior. Considering the formation of FN-collagen complexes is mainly attributed to hydrophobic interaction, a relatively strong binding,[23] which means FN would be firmly anchored on gelatin surface, we further wonder whether accumulation of FN would affect the differentiation of MSCs. MSCs have the potential to differentiate into neural cells *in vitro*.[24–28] We reported previously that by co-culturing with SCs, MSCs differentiated to neuron-like cells with expression of mature neural markers including synapse related protein *in vitro*.[29–31] Together with the fact is that FN plays an important role during nerve system development.[32,33] In the present study, we aimed to determine whether FN secreted by MSCs after the early days of culture would affect the behavior of differentiating MSCs derived cells and more importantly, whether autocrine FN enriched in the implant would impact on nerve fiber regeneration in a spinal cord transection model. Our findings strongly indicate the dynamic influence of autocrine ECM on cell behavioral and functional changes during cell development and neuronal process regeneration.

## MATERIALS AND METHODS

### Isolation and culture of MSCs

MSCs were isolated as previously described[34] from green fluorescent protein (GFP) transgenic Sprague–Dawley rats (Osaka University, Osaka, Japan) which express ubiquitously GFP in all their tissues. Briefly, one-week-old rats were sacrificed and their femurs were flushed with and then cultured in the low glucose Dulbecco's modified Eagle's medium (L-DMEM; Life Technologies,) supplemented with 10% fetal bovine serum (FBS; TBD Co, Tianjin, China) and 4 mM L-glutamine (Life Technologies) in an incubator with 5% $CO_2$ at 37°C. When the adherent cells grew to 80% confluence they were passaged (1:3) into different culture flasks. MSCs of passages 3–6 were employed for the study.

**Purification of SCs.** Acquisition of SCs was also performed as previous described.[35] Five-day-old Sprague–Dawley neonatal rats were sacrificed by decapitation and cleaned by brief submersion in 70% ethanol. The sciatic nerve and brachial plexus were dissected, and placed in a sterile culture dish containing ice-cold D-Hank's solution without calcium chloride and magnesium chloride, where they were maintained until the nerves had been harvested from all of the rats and epineurial membranes were removed under a dissecting microscope. Nerves were cut into small pieces (< 2 mm) and digested with 0.16% collagenase (Sigma-Aldrich, St. Louis, MO) in 37°C for 15 min. Dissociated cells were plated on poly-D-lysine-coated culture dishes with some DMEM/F12 medium consisting of 10% FBS (TBD). After 30 min, an extra 2 mL of the abovementioned culture medium was added to the existing culture dishes. Cells were maintained in a cell culture incubator at 37°C, with a 5% $CO_2$ humidified atmosphere. The medium was changed every 2 days. The cells were subcultured when the culture dishes were 80% confluent, typically after 5–7 days in culture, depending on the initial SC population size, and the cell proliferation rate. Cells were purified by differential velocity adherent methods. Consistent with our previous work, the purity of the SCs used for seeding the scaffolds was 95–96%

### Coculture of MSCs and SCs in 3D gelatin sponge scaffolds

The construction of 3D gelatin sponge scaffolds was done as previous described.[21] Before seeding of cells, the scaffolds were soaked with the culture medium for 10 min and then excessive fluid was absorbed with a Waterman filter article. A transwell system (Corning, NY) was adopted for the

coculturing design. Briefly, the hanging well insert, with pore size of 0.4 μm was coated with poly-D-lysine (Sigma) 1 day prior to cell seeding. A total of $1\times10^5$ SCs were placed in each well of a 24-well plate, submerged by 500 μL culture medium (DMEM + 10% FBS). Subsequently, a total number of $1\times10^5$ MSCs in 10 μL culture medium were seeded to each GS scaffold. In order to facilitate cell adhesion, scaffolds with implanted MSCs were incubated in humidified atmosphere at 37°C for 15 min in the lower chamber of the 24-well plate (1 scaffold per well) before adding in 1 mL culture medium. The upper insert was then placed inside each well separately and the 24-well plates were kept in a 37°C, 5% $CO_2$ and above 70% humidity incubator for culture. Two groups of cells were designed for this experiment. Three hours later, one group received FN blocking antibodies directed against gelatin binding domain was designated as the M + FNab group. Briefly, For the M + FNab group, 400 ng/mL FN blocking antibodies (gelatin binding domain, mouse origin, clone IST-10, EMD Millipore) in 20 μL culture medium were applied into each well. The other group, namely the M group, received 20 μL culture medium only. The culture medium was half-changed every 2 days for both group and FN blocking antibodies were added on daily basis for the M + FNab group. After 3, 7, or 14 days culture, the scaffolds in each group were fixed by 4% paraformaldehyde in 0.1 M PBS (pH 7.4), and then frozen and embedded in the optimum cutting temperature (OCT) compound (Sakura Finetek, Zoeterwoude, The Netherlands). Each sample was cut horizontally at 30 μm thickness for regular immunofluorescence cytochemical staining (IFC) or 60 μm thickness for IFC and 3-dimensional reconstruction study (See below for details).

## Spinal cord injury and transplantation

To prepare the spinal cord injury model, adult female Sprague–Dawley rats (220–250 g, supplied by the Experimental Animal Center of Sun Yat-sen University, China) were used. The animals were anesthetized with 1% pentobarbital sodium (40 mg/kg, i.p.). A laminectomy was carried out to expose the T9 and T10 spinal cord segments, and the dura was cut vertically with a pair of microforceps and microscissors. A pair of angled microscissors were used to fully transect the spinal cord, and a 2-mm segment of the spinal cord at the level T10 was removed. After thorough hemostat, the scaffold with MSCs in transwell coculture system from either the M group ($n = 8$) or the M + FNab group ($n = 8$) was implanted into the injury gap of spinal cord. After the surgical incisions were sutured, the rats received extensive post-operation care including intramuscular injection of penicillin (50,000 U/kg/d) for 3 days and manual emiction two to three times daily till their automatic micturition function was reestablished. Four weeks later, all animals were terminated for histological evaluation. All experimental protocols and animal handling procedures were approved by the Animal Care and Use Committee of Sun Yat-sen University, and were consistent with the National Institutes of Health Guide for the Care and Use of Laboratory Animals.

## Immunofluorescence cytochemical staining

For in vitro study, samples were immunofluorescently stained for FN (Polyclonal IgG from Rabbit, EMD Millipore), Laminin (LN, Boster, Wuhan, China), Vitronectin (VN, Boster), and NG2 (a chondroitin sulfate proteoglycan, EMD Millipore) Neurofilament-150 (NF, Sigma), Intergrin-β1 (EMD Millipore), β-III tubulin (Sigma). For in vivo study, rats were perfused with 4% paraformaldehyde and their spinal cord were dissected, embedded in OTC and horizontally sectioned into 30-μm-thick slices. Primary antibodies including those targeting against FN (Polyclonal IgG from Rabbit, EMD millipore), NF (Sigma) and growth associated protein-43 (GAP-43, Sigma) were used for in vivo study. After blocking with 10% goat serum, the respective primary antibodies were used along with Cy3, DyLight™405-tagged goat IgG or DyLight™649-tagged goat IgG as the secondary antibody (Jackson ImmunoResearch). Hoechst33342 was used for counterstaining of nucleus as necessary. The sections were observed and imaged under the confocal microscope (Carl Zeiss, Germany). For 3D reconstruction, Z stack scanning was first performed, followed by image processing with Zen 2012 software (Carl Zeiss).

## Transmission electron microscopy

For transmission electron microscopy (TEM), scaffolds in the M group after 14 days culture were fixed with 4% PFA for 1 h, followed by vibratome sectioning. Each tissue slice was cut at 100 μm thickness. Tissue slices were placed in 25% sucrose plus 10% glycerol solution for 4 h before freezing and thawing with liquid nitrogen. Slices were blocked by 5% BSA for 1 h and incubated with FN antibody (Polyclonal IgG from Rabbit, EMD Millipore) for 12 h at 4°C and then with 1.6 nm gold particle labeled secondary antibody for 2 h in room temperature. An 8 min silver enhancement staining was carried out after rinsing 3 times in TBS. The slices were then fixed in 2.5% glutaraldehyde for 1 h at 4°C and postfixed with 1% osmic acid for 1 h. Scaffolds were dehydrated through graded ethanol and embedded in an epon mixture overnight, followed by polymerization for 48 h at 60°C. Ultrathin sections were cut with an ultramicrotome (Reichert E, Co, Vienna, Austria) and examined under a transmission electron microscope (Philips CM 10, Eindhoven, Holland).

## Scanning electron microscopy

The cells on the scaffolds in either the M or M + FNab groups after 14 days culture were examined by scanning electron microscopy (SEM). For SEM, scaffolds were firstly washed 3 times with PBS, fixed in 2.5% glutaraldehyde overnight, dehydrated with a series of graded ethanol, and then freeze dried for 2 days. The dried samples were coated with gold and examined under a scanning electron microscope (Philips XL30 FEG).

## Reverse transcriptase-polymerase chain reaction analysis

For total RNA extraction, samples ($n = 4$) from the M + S group at either 3, 7, or 14 days after coculture were washed
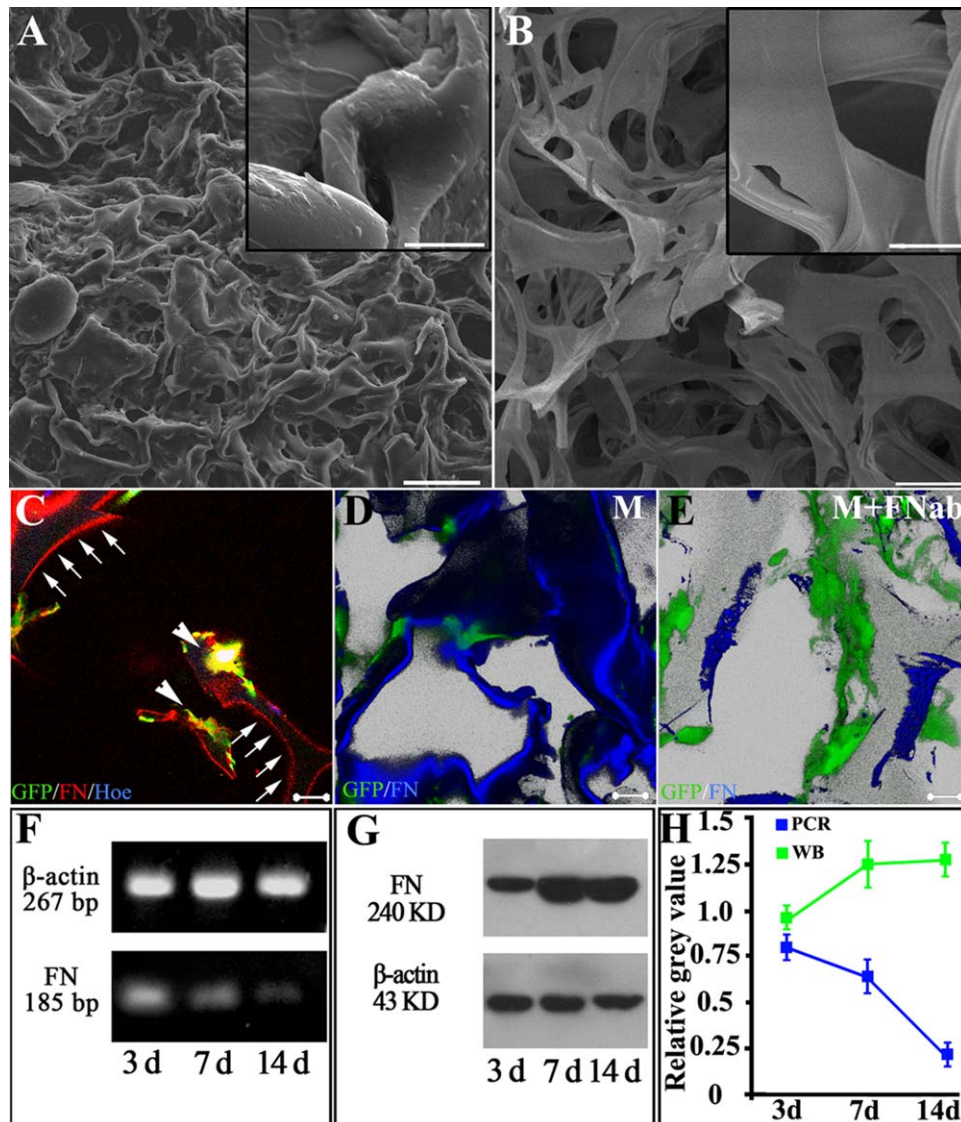
**FIGURE 1**. Fibronectin deposition on the surface of gelatin material after co-culture of MSCs and SCs. ECM accumulation is significant in gelatin sponge (GS) in the MSCs group (A), as evidenced by the rough surface (inset in A), while the surface of GS without MSCs is smooth (inset in B). FN, secreted by GFP positive MSCs (arrowheads in C), deposits onto the surface of gelatin material and displays thread-like red fluorescence (arrows in C). Application of FN antibody decreases the deposition of FN onto the surface of gelatin material. Three dimensional reconstructive image shows that the surface of gelatin material is decorated by adherent FN (blue, in D). After adding FN blocking antibody (FNab) to the culture medium, deposition of FN (blue) onto the surface is obviously reduced as shown in (E). Green cells in D and E are MSCs. RT-PCR and Western blot results indicate that, although the transcriptional level of FN decreases with the increase in duration of co-culture (F), the amount of FN protein increases within the gelatin sponge (GS) scaffolds (G,H). Scale bars: 200 $\mu$m in (A,B), 20 $\mu$m in the inset of (A,B), and 20 $\mu$m in (C–E).

twice with PBS. Then, 1 mL of Trizol (Invitrogen) was added. After adding 200 $\mu$L of chloroform and shaking vigorously for 15 s, the mixture was left in ice for 5 min. The mixture was next centrifuged for 15 min at 12,000 rpm at 4°C. After the supernatant was transferred to a 1.5 mL tube, an equal amount of isopropyl alcohol was added, and the mixture was left at −20°C for 10 min. At 4°C the mixture was centrifuged again for 15 min at 12,000 rpm. The supernatant was re moved and washed with 1 mL of 75% ethanol. The solution was centrifuged once again for 10 min in 12,000 rpm at 4°C, and the supernatant was removed. RNA pellet was dried at room temperature for 10–20 min. It was dissolved into DEPC-water and left for 10 min at 55–60°C.

PrimeScriptTMRT reagent (Takara, Japan) was used for cDNA synthesis following the manufacturer's instructions. Then, using each synthesized cDNA as a mould, PCR by using Prime Script II High Fidelity Reverse transcriptase-polymerase chain reaction (RT-PCR) Kit (Takara) was performed with the FN primers with Forward strand: 5′-GGCTCAATCCAAATGCCTCTAC-3′ and Reverse strand: 5′-CCCTCTGGTAAGGCCAGTCAG-3′, while β-actin with Forward strand: 5′-AGAGGGAAATCGTGCGTGAC-3′ and Reverse strand: 5′-AGAGGTCTTTACGGATGTCAACG-3′ as loading reference. A total of 30 cycles were carried out. After this, electrophoresis was performed on the DNA fragments synthesized by PCR using 2% agarose gel on 0.5 × TBE buffer
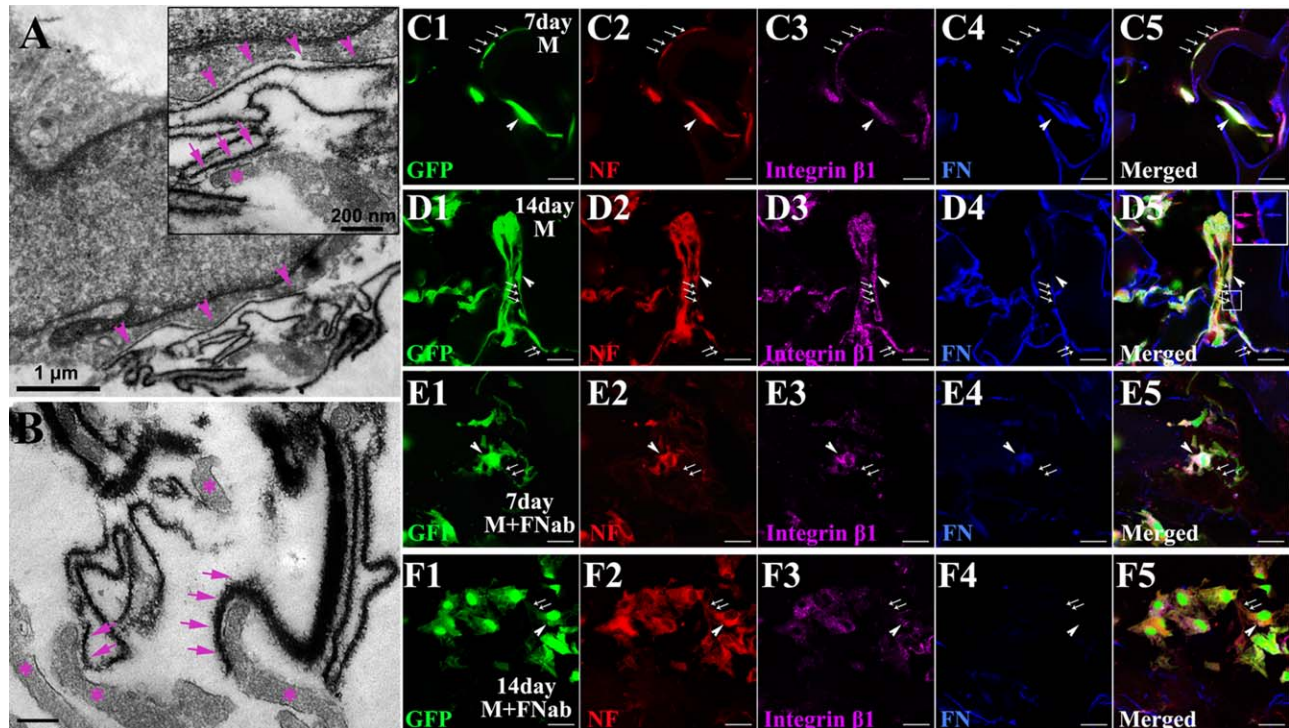
**FIGURE 2.** Cell processes adhere to FN via integrin β1. By immunoelectron microscopy, silver-enhanced nanogold labeled FN shows as dark thread-like line of varying thickness and length (arrows in A,B). Cell membrane (arrowheads in A and the inset of A for enlargement) adheres directly onto FN (arrows in the inset of A) and the cell processes (asterisks in the inset of A and in B) elongate along the FN line (arrows in B). When cocultured with SCs in a transwell system for 7 days, MSCs (green, arrows for cell processes and arrowhead for cell body) differentiate into neuron-like cells bearing NF positive long processes (red, arrows), which adhere to FN (blue, arrows and arrowhead) coating the surface of gelatin material (C1–C5). Their processes grow longer when they are being cultured for additional 7 days (D1–D5). Most of these processes extend along FN line (D2) and (D4) with integrin β1 (purple, arrows, and arrowhead in (D3–D5) and the insert in (D5) for enlarged view). But when cultured in medium added with FN blocking antibody (FNab), MSCs differentiate into NF positive neuron-like cells with shorter processes (arrows), whether for 7 (E1-E5) or 14 days (F1-F5). Note that these cells lack integrin β1 in their short processes (arrows in E3,F3). Scale bar: 1 μm in (A); 200 nm in the inset of (A) and in (B); and 20 μm in (C)–(F).

under 100 V. It was stained with SYBR green and observed under a U.V. illuminator (Syngene, UK).

### Electrophoresis and Western blot

The amount of FN in each group was determined by electrophoresis and Western blot analysis. At different time points (3, 7, and 14 days for FN) in culture, 3 scaffolds from each group were rinsed 3 times in warm D-Hank's solution to remove the residual culture medium, and then cut into small pieces with a pair of eye scissors. These small pieces were immersed in 100 μL lysis buffer containing 1 μL protease inhibitor cocktails for 20 min on ice and dissociated by an ultrasonic homogenizer to dissolve intracellular and extracellular proteins. The lysates were centrifuged at 14,000 rpm for 20 min at 4°C. After a Bradford protein assay (Bio-Rad), equal amounts of the protein suspension were loaded on a 10% polyacrylamide gel, separated by gel electrophoresis, and transferred onto a polyvinylidene fluoride (PVDF) membrane (Millipore, MA). After blocking with 10% non-fat milk in TBST (25 mMTris-HCl, 0.15 M NaCl, and 0.1% Tween 20) for 1 h, membranes were incubated with the according primary antibodies at 4°C overnight. After washes with PBS plus 0.1% Tween-20, membranes were incubated with the horseradish peroxidase (HRP)-con-

jugated secondary antibody (Jackson ImmunoResearch) for 2 h. Finally, membranes were washed again and the bands were detected with an ECL Western blot substrate kit (Pierce, IL).

### Morphological quantification and statistical analysis

For quantification of the percentages of positive cells *in vitro*, one in every ten of the whole series of transverse sections from each scaffold was selected. After being immunofluorescently stained with respective markers, five counting frames at the magnification of 10× or 40× were randomly chosen for each of the sections. The percentage of β-III tubulin or NF positive cells was calculated by counting total number of β-III tubulin or NF positive cells, and dividing the result by total number of GFP positive cells selected.

For quantification of neuronal process length *in vitro*, cells in 45 counting frames under at 40× objective (approximately 360–400 cells) were counted. The 3D reconstruction and neuronal process length measurement were carried out by Imaris 3.0 (Bitplane, Zurich, Switzerland).

To assess innervation of the injury/graft site of spinal cord, Image-Pro Plus software (MediaCybernetics, Silver Spring, MD) was used as described previously.[31] One in every ten spinal cord longitudinal sections from each animal
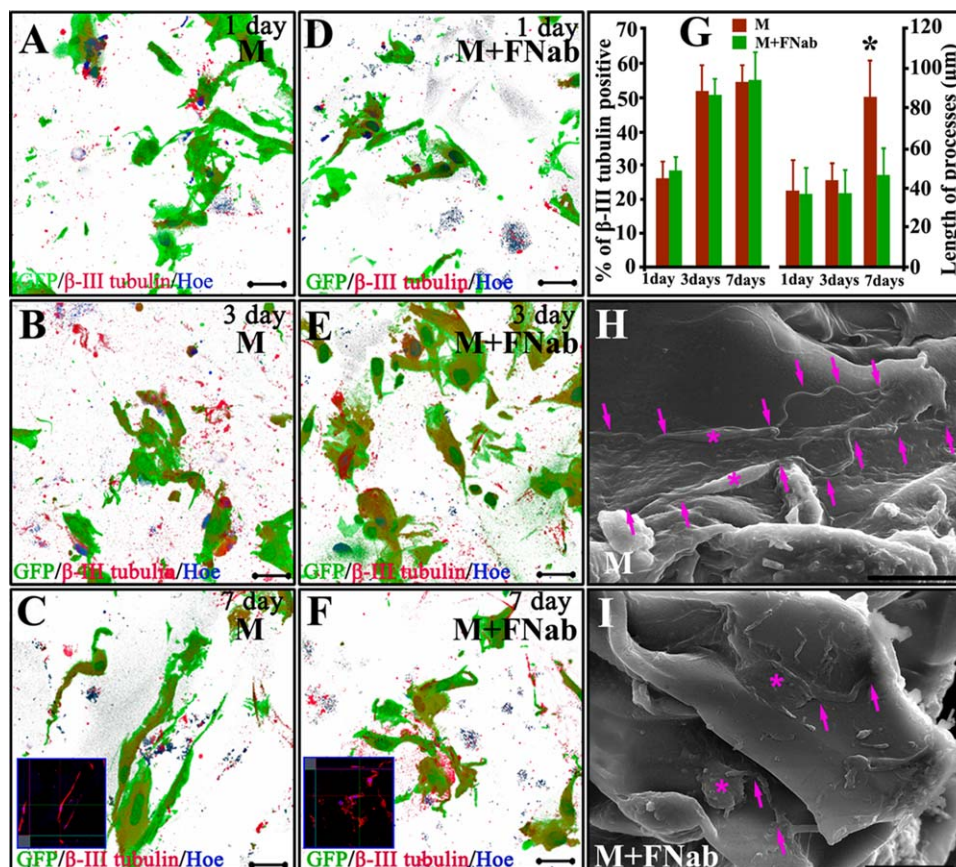
**FIGURE 3**. Three dimensional reconstruction images show neuronal differentiation and neurite length without/with FN blocking antibody (FNab) application. Neuronal neurites grow longer with increase in culture days (A–C). Elongation of neurites is not obvious after application of FN blocking antibody (D–F). Statistical analysis reveals that, application of FN blocking antibody does not affect neuronal differentiation of MSCs, but it attenuates neuron-like cells to elongate their neurites (G). SEM shows neuron-like cell morphology on 3D gelatin sponge scaffolds. At 14 days after culture, most MSCs-derived cells with a spindle-shaped cell body (asterisks in H) protrude thin and long processes perching on the surface of gelatin material (arrows in H). Following FN antibody blocking (asterisks in I), MSCs-derived cells exhibit a flatter cell body, and shorter and thicker processes (arrows in I). Scale bars: 20 μm in (A–F), (H,I). Asterisk in (G) indicates $p < 0.05$ ($n = 9$, Student $t$-test).

was processed. Five randomized $0.7 \times 0.5$ mm$^2$ areas from the rostral interface between the host tissue and the implant, the central area of the implant and the caudal interface between the host tissue and the implant for each of the sections were scrutinized. NF positive never fibers were converted to an area of interest (AOI) and pixel area of each AOI was automatically calculated by the software.

All statistical analyses were performed using the statistical software SPSS11.0. Data were reported as means ± standard deviations (SD). The data were analyzed using Student's $t$ test. The significant level was set at 0.05.

## RESULTS

### FN deposition on GS surface

To demonstrate the specific adherent property of FN to gelatin material, MSCs inside a scaffold and SCs were co-cultured in a transwell system for 7 days. Under SEM, the topology feature of the GS surface changed dramatically with MSCs residing inside [Fig. 1(A)], compared with GS without MSCs seeding [Fig. 1(B)]. ECM accumulation was significant in GS with the MSCs group, as evidenced by the

rough surface [inset in Fig. 1(A)], while the surface of GS without MSCs was smooth [inset in Fig. 1(B)]. IFC staining was then carried out to detect the immunofluorescence signal emitted from different ECM components. As shown in Figure 1(C), only FN adhering to the surface of GS formed thread-like structures with emitted fluorescence and were deposited on the outer layer in a cross section of a gelatin sponge fiber. Remarkably, neither VN [Supporting Information Fig. 1(A)] nor NG2 [Supporting Information Fig. 1(B)] adhered onto GS. To better evaluate the extent of FN accumulation, FN blocking antibodies were applied to prevent the deposition of FN. Three dimensional reconstruction of IFC staining image shows abundant FN deposition on GS surface [Fig. 1(D)]; however, such a distribution pattern was attenuated after application of FN blocking antibodies against gelatin binding domain [Fig. 1(E)].

Accumulation of FN secreted by MSCs in the scaffolds was examined at both mRNA and protein levels. RT-PCR showed that FN mRNA levels in MSCs decreased with the passage of time [Fig. 1(F)]; conversely, the expression of FN protein within the scaffold material was progressively increased [Fig. 1(G)].

## FN facilitates the attachment of cell process through binding with integrin β1

TEM showed direct attachment of cell processes to FN. Silver enhanced nano-gold labeled FN showed thread like structures that were highly electron dense, on which the cell membrane formed direct attachment, suggesting FN may facilitate cell adhesion [Fig. 2(A)]. The FN fibers varied in diameter and length indicating the variation in assembling pattern of FN molecules. Interestingly, the cell processes followed the contours of FN [asterisks in Fig. 2(B)].

To further determine if cell attachment to FN was mediated by integrin β1, cell containing scaffolds were cultured for 7 or 14 days with or without FN antibody treatment [Fig. 2(C–F)]. In agreement with our previous SCs induced neuronal differentiation result,[31] MSCs differentiated into neuron-like cells with long extending NF positive processes, closely adherent to FN decorated gelatin scaffolds. The processes increased in length when cultured for 14 days [Fig. 2(D1–D5)]. These cell processes appeared to co-express integrin β1 [Fig. 2(D3)]. However, when cultured in medium with added FN antibody, MSCs differentiated into NF positive neuron-like cells with short processes in 7 or 14 days cultures [Fig. 2(E,F)]. The processes lacked integrin β1 expression suggesting that it plays an important role FN induced cell attachment.

## Autocrine FN promotes cell process elongation

Three dimensional images were used to quantify the neuronal differentiation percentage and process length with/without blocking with FN antibody. Neuronal processes grew longer with increase in duration in culture [Fig. 3(A–C)]. Elongation of neuronal processes became less obvious following FN blockade with its antibody to eliminate their binding to gelatin surface [Fig. 3(D–F)]. FN antibody treatment did not affect neuronal differentiation of MSCs, but it decreased elongation of the processes [Fig. 3(G)].

Moreover, FN also changed the external morphology of MSC-derived neuron-like cell as shown by SEM, which revealed the external neuron-like cell morphology on 3D gelatin sponge scaffolds. After 14 days culture, most MSC-derived cells exhibited a spindle shaped cell body [Fig. 3(H)] with projection of slender and long processes by adhering to the surface of gelatin scaffold [arrows in Fig. 3(H)]. Following FN antibody treatment, MSC-derived cells showed a flattened cell body [asterisks in Fig. 3(I)], and shorter and thicker processes [arrows in Fig. 3(I)].

## Autocrine FN increases nerve fiber regeneration *in vivo*

Scaffolds containing MSCs with or without FN blocking antibody treatment for 14 days of culture were transplanted into the injured spinal cord for 4 weeks. The results showed that a large numbers of NF positive and bulky nerve fibers varying in lengths, were observed in the M group [Fig. 4(A)]. These regenerating nerve fibers had a tendency to grow toward the implant [Fig. 4(A1)]. Conversely, significantly fewer NF positive nerve fibers were observed in the M + FNab group [Fig. 4(B)] and these fibers grew in a haphazard manner [Fig. 4(B1)]. A marked increase in
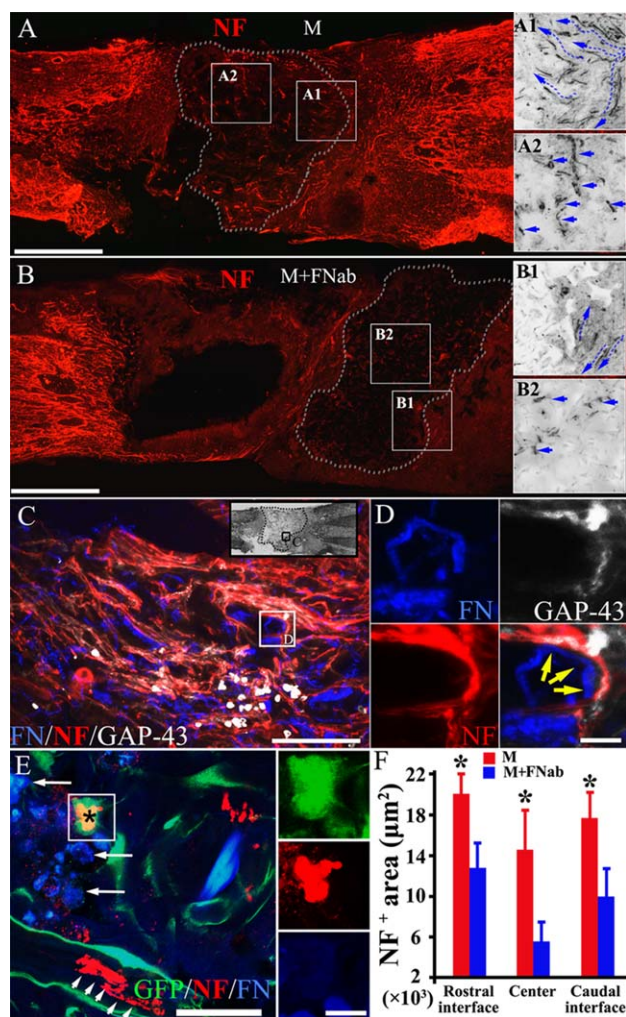


FIGURE 4. Autocrine FN increases nerve fiber regeneration after spinal cord injury. Scaffolds containing MSCs with or without FN blocking antibody treatment for 14 days of culture are transplanted into the injured spinal cord for 4 weeks. NF positive nerve fibers (red), which are bulky and of varying lengths, are observed in the M group (A). These regenerating nerve fibers grow preferentially toward the implant (A1). NF positive fibers are common and are readily identified in the center of the implant (A2). When implanted with FN blocking antibodies treated scaffold, NF positive nerve fibers (B) are uncommon and often in disarrays (B1). They are rarely seen in the center (B2) of the implant in the M + FNab group when compared with the same area (A2) of the M group. Autocrine FN was detected at 4 weeks after implantation, as indicated by the presence of many thread-like fluorescent short fibers in the injury/graft site of spinal cord (C). Nerve fibers attached to FN fibers are common (yellow, arrows in D), with some of them being GAP-43 positive, suggesting robust nerve fiber regeneration in the FN enriched area (C,D). MSC-derived neuron-like cells (red, asterisk of E) can be found inside the implant, surrounded by a significant group of GFP positive donor cells expressing FN (blue). There are a few NF positive nerve fibers (red, arrowheads in E) near the donor cells (GFP positive, in E). FN accumulation in the extracellular space is observed inside the implant (arrows in E). Histogram chart shows a prominent increase of innervation at the rostral interface between the host tissue and implant, the center of the implant and the caudal interface between the host tissue and implant in the M group, compared with the M + FNab group. Asterisks in (F) indicate $p < 0.05$ ($n = 8$, Student $t$-test). Scale bars: 1 mm in (A) and (B); 200 μm in (C); 20 μm in (D); 50 μm in (E); 10 μm in inset of (E).

regenerating nerve fibers was observed in the epicenter of M group [Fig. 4(A2)], compared with the M + FNab group [Fig. 4(B2)]. The overall innervation of the rostral interface, the epicenter and the caudal interface of the implants was significantly higher in M group than in M + FNab group [Fig. 4(F)]. We reported previously that deposited FN was detected on GS scaffold at least one week after implantation in the spinal cord.[21] In this study over a protracted time period in the spinal cord, autocrine FN was detected at 4 weeks after implantation. This is evidenced by the existence of many thread-like fluorescent short nerve fibers (red) in the injury/graft site [Fig. 4(C)] notably in the M group. Many profiles of nerve fibers were adherent to the FN fibers [Fig. 4(C)], and very strikingly some of them were GAP-43 positive, suggesting robust nerve fiber regeneration in the FN enriched area [Fig. 4(C,D)]. Consistent with our previous finding,[36] the neuronal differentiation of MSCs decreased drastically 4 weeks after their transplantation into the spinal cord tissue. The percentage of NF positive neuron-like cells was $5.74 \pm 2.25\%$ for the M group and $6.68 \pm 3.22\%$ for the M + FNab group ($p > 0.05$, $n = 8$, Student's $t$-test). Majority of the GFP positive donor cells were found to express FN that accumulated in the extracellular spaces [Fig. 4(E)], and which would induce NF positive host nerve fiber growth [Fig. 4(E)]. Figure 4(F) shows a more substantial increase of innervation area in the rostral and caudal interfaces between the host tissue and the injury/graft site as well as the center of the injury/graft site of spinal cord in the M group, when compared with the M + FNab group.

## DISCUSSION

Previous studies demonstrated that SCs were able to induce neural differentiation of MSCs,[29,37] probably due to their remarkable capacity of cytokines secreting such as brain derived neurotrophic factor (BDNF), neurotrophin-3 (NT-3), basic fibroblast growth factor (bFGF) and glial cell line-derived neurotrophic factor (GDNF),[38] which were considered to be effective trophic factors for neural induction of MSCs.[28,39] Compared with our previous 2D study,[29] MSCs on a gelatin sponge scaffold resulted in more neuronal differentiation under the SCs induction. We attribute this increase to the benefit of 3D culture system[40–42] and also the soft nature of gelatin,[43] which was deemed to be more comparable to the elastic nature of the CNS tissue[44] and hence could be neurogenic.[45] With the differentiation of MSCs into neuron-like cells, the expression of FN was concomitantly and progressively decreased. This may be a possible result of switching of the cell type from mesodermal to ectodermal due to a decreased expression of mesoderm gene in cells undergoing neural differentiation.[46,47] Although RT-PCR showed an obvious reduction in FN expression, the amount of FN protein within the scaffold increased with time. This observation was consistent with our previous finding that gelatin could accumulate FN[21] due to their binding via the GBD domain.[22] Since this binding is relatively strong as it even resists normal detergents,[23] almost the entire surface of gelatin sheet was covered by FN fibrils.

Although MSCs are able to secrete matrix metalloproteinase (MMP) such as MMP2 that may degrade ECM including FN and migrate away,[48,49] we believe in the present study the accumulation effect had overridden the degradation effect as indicated by the fact that a broad FN-coated surface was gradually formed.

In the 3D GS culture system, catabolic process of FN is apparently different from *in vivo* situation, where existence of FN is highly regulated by gene from manufacturing to degradation.[50,51] However, the system provided a unique platform for exploring the promising prospects of MSCs in tissue engineering field. Although there are many reports showing the neuronal differentiation of MSCs,[24–28] less attention has been paid to neurite elongation, which is the first step for neuron maturation, along with formation of synaptic contacts and neural network. The present results did not provide sufficient evidence to conclude that FN can increase neuronal differentiation of MSCs. However, we did observe that FN had impact on the neurite outgrowth from MSC-derived neuron-like cells, probably through combination with its receptor β1 integrin. FN is known to act as a ligand for at least 11 different integrin heterodimers,[52] supporting adhesion of numerous cell types and also neurite outgrowth from developing peripheral nervous system and central nervous system (CNS) neurons.[33,53,54] While in the adult animals, peripheral nerve injury could up-regulate FN expression.[55,56] The integrin β1 is expressed on regenerating axons [55,57] as suggested by *in vitro* neurite prolongation from dorsal root ganglion neurons on FN substrate.[58] In CNS, integrin β1 is expressed by neurons during development and mature neurons in the hippocampus and cerebral cortex.[59] During the maturation of brain neurons, integrin β1 expression is down-regulated [60] to lower but still detectable level.[61] The temporally regulated expression pattern of integrin ensures correct migration, differentiation and network formation of neurons during the maturation process. Consistent with these findings, we show here that NF positive neural processes adhered to FN-decorated scaffold through integrin β1 receptors and more importantly, blocking the cell-binding domain of FN resulted in decrease of integrin β1. Antibodies directed against the gelatin binding fragment of fibronectin inhibited fibronectin deposition on GS and subsequently, integrin binding by fibronectin and possible downstream signal transduction events would also be influenced.[62] Classic synaptogenesis is evident by the occurrence of neurites which appeared to make synaptic-like contacts as well as the formation of pre-synaptic component and the inducible post-synaptic component with their associated proteins, it is therefore suggested that the mutual contact of neurites is the structural basis for synapse formation.[63] Separately, a drastic shortening in length of neurites was observed on the gelatin sponge scaffold without FN matrix support. It is conceivable that this would result in a significant reduction in post-synaptic protein expression; hence, formation of fewer synaptic contacts. Moreover, decreased expression of integrin β1 could directly reduce synapse density and maturation,[64,65] which resulted in a lesser neural network formation. It is well established

that growing neuronal processes remain stable if they form synapses with the targets and receive trophic factors retrogradely transported from the post-synaptic component.[66,67] The significantly increased amount and the growth pattern of regenerating nerve fibers in the current study suggests that autocrine FN, deposited on the surface of GS, may facilitate nerve regeneration through providing a permissive matrix.[68,69]

## CONCLUSION

This study assessed the influence of FN on the neurite outgrowth from MSC-derived neuron-like cells and differentiating MSCs in the gelatin sponge scaffold. Our results suggest that collagen-origin substrate, gelatin material, can accumulate FN beginning from the stem cell phase of MSCs, till specifically differentiated phase which could affect profoundly cell process elongation. The data further indicate that adhesion of ECM onto the surface of scaffold would have a significant influence on cell behavior during the development of stem cells as well as nerve fiber regeneration when introduced into a spinal cord injury model. All this should be taken into consideration when designing a specific biomaterial scaffold for tissue engineering construction.

## REFERENCES

1. Yamada KM. Cell surface interactions with extracellular materials. Annu Rev Biochem 1983;52:761–799.
2. Adams JC, Watt FM. Regulation of development and differentiation by the extracellular matrix. Development 1993;117:1183–1198.
3. Behrendtsen O, Alexander CM, Werb Z. Cooperative interactions between extracellular matrix, integrins and parathyroid hormone-related peptide regulate parietal endoderm differentiation in mouse embryos. Development 1995;121:4137–4148.
4. Moore KA, Lemischka IR. Stem cells and their niches. Science 2006;311:1880–1885.
5. Maisel M, Habisch HJ, Royer L, Herr A, Milosevic J, Hermann A, Liebau S, Brenner R, Schwarz J, Schroeder M, Storch A. Genome-wide expression profiling and functional network analysis upon neuroectodermal conversion of human mesenchymal stem cells suggest HIF-1 and miR-124a as important regulators. Exp Cell Res 2010;316:2760–2778.
6. Chen XD, Dusevich V, Feng JQ, Manolagas SC, Jilka RL. Extracellular matrix made by bone marrow cells facilitates expansion of marrow-derived mesenchymal progenitor cells and prevents their differentiation into osteoblasts. J Bone Miner Res 2007;22:1943–1956.
7. Wakitani S, Imoto K, Yamamoto T, Saito M, Murata N, Yoneda M. Human autologous culture expanded bone marrow mesenchymal cell transplantation for repair of cartilage defects in osteoarthritic knees. Osteoarthritis Cartilage 2002;10:199–206.
8. Kundu AK, Khatiwala CB, Putnam AJ. Extracellular matrix remodeling, integrin expression, and downstream signaling pathways influence the osteogenic differentiation of mesenchymal stem cells on poly(lactide-co-glycolide) substrates. Tissue Eng Part A 2009;15:273–283.
9. Chen XD. Extracellular matrix provides an optimal niche for the maintenance and propagation of mesenchymal stem cells. Birth Defects Res C Embryo Today 2010;90:45–54.
10. Yoshimura K, Suga H, Eto H. Adipose-derived stem/progenitor cells: Roles in adipose tissue remodeling and potential use for soft tissue augmentation. Regen Med 2009;4:265–273.
11. Cherubino M, Marra KG. Adipose-derived stem cells for soft tissue reconstruction. Regen Med 2009;4:109–117.
12. Laco F, Kun M, Weber HJ, Ramakrishna S, Chan CK. The dose effect of human bone marrow-derived mesenchymal stem cells on epidermal development in organotypic co-culture. J Dermatol Sci 2009;55:150–160.
13. Ma K, Laco F, Ramakrishna S, Liao S, Chan CK. Differentiation of bone marrow-derived mesenchymal stem cells into multi-layered epidermis-like cells in 3D organotypic coculture. Biomaterials 2009;30:3251–3258.
14. Kwon SH, Lee TJ, Park J, Hwang JE, Jin M, Jang HK, Hwang NS, Kim BS. Modulation of BMP-2-induced chondrogenic versus osteogenic differentiation of human mesenchymal stem cells by cell-specific extracellular matrices. Tissue Eng Part A 2013;19:49–58.
15. Yurchenco PD, Tsilibary EC, Charonis AS, Furthmayr H. Models for the self-assembly of basement membrane. J Histochem Cytochem 1986;34:93–102.
16. Martin GR, Timpl R. Laminin and other basement membrane components. Annu Rev Cell Biol 1987;3:57–85.
17. Mao Y, Schwarzbauer JE. Stimulatory effects of a three-dimensional microenvironment on cell-mediated fibronectin fibrillogenesis. J Cell Sci 2005;118:4427–4436.
18. Ohno M, Motojima K, Okano T, Taniguchi A. Maturation of the extracellular matrix and cell adhesion molecules in layered co-cultures of HepG2 and endothelial cells. J Biochem 2009;145:591–597.
19. Matsusaki M, Ajiro H, Kida T, Serizawa T, Akashi M. Layer-by-layer assembly through weak interactions and their biomedical applications. Adv Mater 2012;24:454–474.
20. Tibbitt MW, Anseth KS. Dynamic microenvironments: The fourth dimension. Sci Transl Med 2012;4:160ps24.
21. Zeng X, Zeng YS, Ma YH, Lu LY, Du BL, Zhang W, Li Y, Chan WY. Bone marrow mesenchymal stem cells in a three-dimensional gelatin sponge scaffold attenuate inflammation, promote angiogenesis, and reduce cavity formation in experimental spinal cord injury. Cell Transplant 2011;20:1881–1899.
22. Balian G, Click EM, Bornstein P. Location of a collagen-binding domain in fibronectin. J Biol Chem 1980;255:3234–3236.
23. Gold LI, Pearlstein E. Fibronectin-collagen binding and requirement during cellular adhesion. Biochem J 1980;186:551–559.
24. Schultz SS, Lucas PA. Human stem cells isolated from adult skeletal muscle differentiate into neural phenotypes. J Neurosci Methods 2006;152:144–155.
25. Qian L, Saltzman WM. Improving the expansion and neuronal differentiation of mesenchymal stem cells through culture surface modification. Biomaterials 2004;25:1331–1337.
26. Abouelfetouh A, Kondoh T, Ehara K, Kohmura E. Morphological differentiation of bone marrow stromal cells into neuron-like cells after co-culture with hippocampal slice. Brain Res 2004;1029:114–119.
27. Cho KJ, Trzaska KA, Greco SJ, McArdle J, Wang FS, Ye JH, Rameshwar P. Neurons derived from human mesenchymal stem cells show synaptic transmission and can be induced to produce the neurotransmitter substance P by interleukin-1 alpha. Stem Cells 2005;23:383–391.
28. Trzaska KA, King CC, Li KY, Kuzhikandathil EV, Nowycky MC, Ye JH, Rameshwar P. Brain-derived neurotrophic factor facilitates maturation of mesenchymal stem cell-derived dopamine progenitors to functional neurons. J Neurochem 2009;110:1058–1069.
29. Zhang YQ, Zeng X, He LM, Ding Y, Li Y, Zeng YS. NT-3 gene modified Schwann cells promote TrkC gene modified mesenchymal stem cells to differentiate into neuron-like cells in vitro. Anat Sci Int 2010;85:61–67.
30. Zhang YQ, He LM, Xing B, Zeng X, Zeng CG, Zhang W, Quan DP, Zeng YS. Neurotrophin-3 gene-modified Schwann cells promote TrkC gene-modified mesenchymal stem cells to differentiate into neuron-like cells in poly(lactic-acid-co-glycolic acid) multiple-channel conduit. Cells Tissues Organs 2012;195:313–322.
31. Zeng X, Qiu XC, Ma YH, Duan JJ, Chen YF, Gu HY, Wang JM, Ling EA, Wu JL, Wu W, Zeng YS. Integration of donor mesenchymal stem cell-derived neuron-like cells into host neural network after rat spinal cord transection. Biomaterials 2015;53:184–201.
32. Humphries MJ, Akiyama SK, Komoriya A, Olden K, Yamada KM. Neurite extension of chicken peripheral nervous system neurons on fibronectin: Relative importance of specific adhesion sites in the central cell-binding domain and the alternatively spliced type III connecting segment. J Cell Biol 1988;106:1289–1297.
33. Akers RM, Mosher DF, Lilien JE. Promotion of retinal neurite outgrowth by substratum-bound fibronectin. Dev Biol 1981;86:179–188.

34. Ding Y, Yan Q, Ruan JW, Zhang YQ, Li WJ, Zhang YJ, Li Y, Dong H, Zeng YS. Electro-acupuncture promotes survival, differentiation of the bone marrow mesenchymal stem cells as well as functional recovery in the spinal cord-transected rats. BMC Neurosci 2009;10:35

35. Zeng YS, Ding Y, Wu LZ, Guo JS, Li HB, Wong WM, Wu WT. Co-transplantation of schwann cells promotes the survival and differentiation of neural stem cells transplanted into the injured spinal cord. Dev Neurosci 2005;27:20–26.

36. Qiu XC, Jin H, Zhang RY, Ding Y, Zeng X, Lai BQ, Ling EA, Wu JL, Zeng YS. Donor mesenchymal stem cell-derived neural-like cells transdifferentiate into myelin-forming cells and promote axon regeneration in rat spinal cord transection. Stem cell Res Ther 2015;6:105.

37. Zurita M, Vaquero J, Oya S, Miguel M. Schwann cells induce neuronal differentiation of bone marrow stromal cells. Neuroreport 2005;16:505–508.

38. Azanchi R, Bernal G, Gupta R, Keirstead HS. Combined demyelination plus Schwann cell transplantation therapy increases spread of cells and axonal regeneration following contusion injury. J Neurotrauma 2004;21:775–788.

39. Zurita M, Vaquero J, Oya S, Bonilla C, Aguayo C. Neurotrophic Schwann-cell factors induce neural differentiation of bone marrow stromal cells. Neuroreport 2007;18:1713–1717.

40. Chan V, Zorlutuna P, Jeong JH, Kong H, Bashir R. Three-dimensional photopatterning of hydrogels using stereolithography for long-term cell encapsulation. Lab Chip 2010;10:2062–2070.

41. Peretz H, Talpalar AE, Vago R, Baranes D. Superior survival and durability of neurons and astrocytes on 3-dimensional aragonite biomatrices. Tissue Eng 2007;13:461–472.

42. Xu T, Gregory CA, Molnar P, Cui X, Jalota S, Bhaduri SB, Boland T. Viability and electrophysiology of neural cell structures generated by the inkjet printing method. Biomaterials 2006;27:3580–3588.

43. Vemuri S. A screening technique to study the mechanical strength of gelatin formulations. Drug Dev Ind Pharm 2000;26:1115–1120.

44. Ozawa H, Matsumoto T, Ohashi T, Sato M, Kokubun S. Comparison of spinal cord gray matter and white matter softness: Measurement by pipette aspiration method. J Neurosurg 2001;95:221–224.

45. Engler AJ, Sen S, Sweeney HL, Discher DE. Matrix elasticity directs stem cell lineage specification. Cell 2006;126:677–689.

46. Bertani N, Malatesta P, Volpi G, Sonego P, Perris R. Neurogenic potential of human mesenchymal stem cells revisited: Analysis by immunostaining, time-lapse video and microarray. J Cell Sci 2005;118:3925–3936.

47. Choi CB, Cho YK, Prakash KV, Jee BK, Han CW, Paik YK, Kim HY, Lee KH, Chung N, Rha HK. Analysis of neuron-like differentiation of human bone marrow mesenchymal stem cells. Biochem Biophys Res Commun 2006;350:138–146.

48. Ries C, Egea V, Karow M, Kolb H, Jochum M, Neth P. MMP-2, MT1-MMP, and TIMP-2 are essential for the invasive capacity of human mesenchymal stem cells: Differential regulation by inflammatory cytokines. Blood 2007;109:4055–4063.

49. Collier IE, Wilhelm SM, Eisen AZ, Marmer BL, Grant GA, Seltzer JL, Kronberger A, He CS, Bauer EA, Goldberg GI. H-ras oncogene-transformed human bronchial epithelial cells (TBE-1) secrete a single metalloprotease capable of degrading basement membrane collagen. J Biol Chem 1988;263:6579–6587.

50. Lee G, Hynes R, Kirschner M. Temporal and spatial regulation of fibronectin in early Xenopus development. Cell 1984;36:729–740.

51. Lukes A, Mun-Bryce S, Lukes M, Rosenberg GA. Extracellular matrix degradation by metalloproteinases and central nervous system diseases. Mol Neurobiol 1999;19:267–284.

52. Leiss M, Beckmann K, Giros A, Costell M, Fassler R. The role of integrin binding sites in fibronectin matrix assembly in vivo. Curr Opin Cell Biol 2008;20:502–507.

53. Carri NG, Perris R, Johansson S, Ebendal T. Differential outgrowth of retinal neurites on purified extracellular matrix molecules. J Neurosci Res 1988;19:428–439.

54. Humphries MJ, Akiyama SK, Komoriya A, Olden K, Yamada KM. Neurite extension of chicken peripheral nervous system neurons on fibronectin: Relative importance of specific adhesion sites in the central cell-binding domain and the alternatively spliced type III connecting segment. J Cell Biol 1988;106:1289–1297.

55. Lefcort F, Venstrom K, McDonald JA, Reichardt LF. Regulation of expression of fibronectin and its receptor, alpha 5 beta 1, during development and regeneration of peripheral nerve. Development 1992;116:767–782.

56. Siironen J, Sandberg M, Vuorinen V, Roytta M. Expression of type I and III collagens and fibronectin after transection of rat sciatic nerve. Reinnervation compared with denervation. Lab Invest 1992;67:80–87.

57. Yanagida H, Tanaka J, Maruo S. Immunocytochemical localization of a cell adhesion molecule, integrin alpha5beta1, in nerve growth cones. J Orthop Sci 1999;4:353–360.

58. Gardiner NJ, Moffatt S, Fernyhough P, Humphries MJ, Streuli CH, Tomlinson DR. Preconditioning injury-induced neurite outgrowth of adult rat sensory neurons on fibronectin is mediated by mobilisation of axonal alpha5 integrin. Mol Cell Neurosci 2007;35:249–260.

59. Bi X, Lynch G, Zhou J, Gall CM. Polarized distribution of alpha5 integrin in dendrites of hippocampal and cortical neurons. J Comp Neurol 2001;435:184–193.

60. Yoshida N, Hishiyama S, Yamaguchi M, Hashiguchi M, Miyamoto Y, Kaminogawa S, Hisatsune T. Decrease in expression of alpha 5 beta 1 integrin during neuronal differentiation of cortical progenitor cells. Exp Cell Res 2003;287:262–271.

61. King VR, McBride A, Priestley JV. Immunohistochemical expression of the alpha5 integrin subunit in the normal adult rat central nervous system. J Neurocytol 2001;30:243–252.

62. Kim S, Bell K, Mousa SA, Varner JA. Regulation of angiogenesis in vivo by ligation of integrin alpha5beta1 with the central cell-binding domain of fibronectin. Am J Pathol 2000;156:1345–1362.

63. Lander AD. Molecules that make axons grow. Mol Neurobiol 1987;1:213–245.

64. Huang Z, Shimazu K, Woo NH, Zang K, Muller U, Lu B, Reichardt LF. Distinct roles of the beta 1-class integrins at the developing and the mature hippocampal excitatory synapse. J Neurosci 2006;26:11208–11219.

65. Warren MS, Bradley WD, Gourley SL, Lin YC, Simpson MA, Reichardt LF, Greer CA, Taylor JR, Koleske AJ. Integrin beta1 signals through Arg to regulate postnatal dendritic arborization, synapse density, and behavior. J Neurosci 2012;32:2824–2834.

66. Barde YA. Trophic factors and neuronal survival. Neuron 1989;2:1525–1534.

67. Harrington AW, Ginty DD. Long-distance retrograde neurotrophic factor signalling in neurons. Nat Rev Neurosci 2013;14:177–187.

68. Gomez TM, Letourneau PC. Filopodia initiate choices made by sensory neuron growth cones at laminin/fibronectin borders in vitro. J Neurosci 1994;14:5959–5972.

69. King VR, Alovskaya A, Wei DY, Brown RA, Priestley JV. The use of injectable forms of fibrin and fibronectin to support axonal ingrowth after spinal cord injury. Biomaterials 2010;31:4447–4456.